

SOME FEATURES OF THE FLOW OF GAS THAT OCCURS AS A RESULT OF THE INTERACTION BETWEEN A SHOCK-WAVE AND A CLOUD OF PARTICLES

S. P. Kiselev and V. P. Kiselev

UDC 532.539

In this paper we investigate the interaction between a shock-wave and a rarefied cloud of particles of finite dimensions. It is shown that, for a subsonic flow of the gas, acceleration of the gas into the cloud of particles occurs behind the shock-wave, while at supersonic velocities the gas is slowed down. The results of calculations are compared with experiment on the slowing down of a supersonic flow in a cloud of particles.

1. Consider a cloud of spherical particles on which a shock-wave is incident from the left (Fig. 1, where x^+ , x_0 , and $x_0 + h$ are the position of the shock-wave and the left and right boundary of the cloud, respectively, h is the thickness of the cloud, and $(m_2 \sim 10^{-3})$, are the regions occupied by the gas and the gas with the particles). It is required to calculate the flow of gas and the particles which occurs as a result of interaction between the shock-wave and the cloud of particles. In this paper the motion of the gas and the particles is described by the model of interpenetrating continua [1, 2]. The volume concentration of the particles in the cloud is assumed to be small ($m_2 \sim 10^{-3}$), and the particles are therefore described by the collisionless kinetic equation, while the gas is described by the equations of a dust-containing gas. This model was investigated in detail in [1, 2], and the system of equations in the one-dimensional case has the form

$$\begin{aligned} \frac{\partial f}{\partial t} + v_2 \frac{\partial f}{\partial x} + \frac{\partial a f}{\partial v_2} + \frac{\partial q f}{\partial T_2} &= 0, \\ f &= f(t, x, v_2, r, T_2), \quad n = \int f dv_2 dr dT_2, \\ m_2 &= \frac{4}{3} \pi \int r^3 f dv_2 dr dT_2, \quad m_1 + m_2 = 1, \\ a &= \frac{v_1 - v_2}{\tau_0} - \frac{1}{\rho_{22}} \frac{\partial p}{\partial x}, \quad \frac{1}{\tau_0} = \frac{3}{4} \frac{\text{Re} \mu}{\rho_{22} d^2} C_d(\text{Re}, M_{12}), \\ C_d(\text{Re}, M_{12}) &= \left(1 + \exp\left(-\frac{0,43}{M_{12}^{4,67}}\right) \right) \left(0,38 + \frac{24}{\text{Re}} + \frac{4}{\sqrt{\text{Re}}} \right), \\ \text{Re} &= \frac{\rho_{11} |v_1 - v_2| d}{\mu}, \quad M_{12} = \frac{|v_1 - v_2|}{a}, \quad a = \sqrt{\frac{\gamma p}{\rho_{11}}}, \\ q &= 2\pi \lambda r \text{Nu} \frac{T_1 - T_2}{c_p m_p}, \quad m_p = \frac{4}{3} \pi r^3 \rho_{22}, \quad \text{Nu} = 2 + 0,6 \text{Re}^{0,5} \text{Pr}^{0,33}, \\ \text{Pr} &= \frac{c_p \mu}{\lambda}, \quad \frac{\partial \varphi}{\partial t} + \frac{\partial H}{\partial x} + \Phi = 0, \quad \rho_1 = \rho_{11} m_1, \\ \varphi &= \begin{pmatrix} \rho_1 \\ \rho_1 v_1 \\ \rho_1 (\mathcal{E}_1 + v_1^2/2) \end{pmatrix}, \quad H = \begin{pmatrix} \rho_1 v_1 \\ \rho_1 v_1^2 + p m_1 \\ \rho_1 v_1 A_1 \end{pmatrix}, \quad \Phi = \begin{pmatrix} 0 \\ \Phi_1 \\ A_2 \end{pmatrix}, \end{aligned} \tag{1.1}$$

Institute of Theoretical and Applied Mechanics, Siberian Division of the Russian Academy of Sciences, 630090 Novosibirsk. Translated from *Prikladnaya Mekhanika i Tekhnicheskaya Fizika*, No. 2, pp. 8-18, March-April, 1995. Original article submitted March 11, 1994.

$$\begin{aligned}
A_1 &= \varepsilon_1 + \frac{pm_1}{\rho_1} + \frac{v_1^2}{2}, & \varepsilon_1 &= cvT_1, & p &= (\gamma - 1)\rho_{11}\varepsilon_1, \\
A_2 &= v_1\Phi_1 + p\left(\frac{\partial m_1}{\partial t} + v_1\frac{\partial m_1}{\partial x}\right) - \Phi_2, \\
\Phi_1 &= -p\frac{\partial m_1}{\partial x} + \int m_p\frac{v_1 - v_2}{\tau_0}f dv_2 dr dT_2, \\
\Phi_2 &= \int m_p\left(\frac{(v_1 - v_2)^2}{\tau_0} - c_s q\right)f dv_2 dr dT_2,
\end{aligned}$$

where $v_1, \rho_{11}, \rho_1, T_1, p, \gamma, \varepsilon_1, m_1$ are the velocity, true density, mean density, temperature, pressure, adiabatic index, specific internal energy, and volume concentration of the gas, $v_2, \rho_{22}, r, T_2, m_2, f, n$ are the velocity, true density, radius, temperature, volume concentration, distribution function, and countable concentration of the particles (the subscript 1 relates to the gas and the subscript 2 relates to the particles), μ, λ, a are the viscosity, thermal conductivity and velocity of sound in the gas, and $Re, Nu,$ and M_{12} are the Reynolds, Nusselt and Mach numbers. The system of equations (1.1) was solved numerically on a computer. The method of calculation is described in [3]; we merely note that the equations for the gas were solved on an Euler grid using an explicit scheme of third-order accuracy, while the kinetic equation was solved in Lagrange variables with the first order of accuracy.

We took as the boundary conditions at the input and output of the channel for the gas the condition of symmetry of $v_1, \rho_{11}, \varepsilon_1$, and for the particles the conditions of absorption. At the initial instant the the cloud consisted of spherical particles of plexiglass and contained three fractions: $m_2^{(1)} = 5 \cdot 10^{-4}$ and $d_1 = 170 \mu\text{m}$, $m_2^{(2)} = 10^{-3}$ and $d = 400 \mu\text{m}$, and $m_2^{(3)} = 5 \cdot 10^{-4}$ and $d = 500 \mu\text{m}$, where $m_2^{(i)}$ and d_i are the volume concentration and diameter of the particles of the i -th fraction. The complete volume concentration of the particles $m_2 = \sum_1^3 m_2^{(i)} = 2 \times 10^{-3}$ determines the fraction per unit volume occupied by the particles. The particles of all three fractions were uniformly distributed over the whole volume of the cloud. When $t = 0$ the transverse dimensions of the cloud $h = 1 \text{ cm}$, the temperature of the particles $T_2^0 = 300 \text{ K}$, and the density of the particles of plexiglass $\rho_{22} = 1.2 \text{ g/cm}^3$. The parameters of the gas at $t = 0$ and $x > x^+$ where $p_0 = 0.1 \text{ atm}$ and $T_0 = 300 \text{ K}$.

2. We will consider two cases corresponding to a weak shock-wave with Mach number $M_0 = 1.75$ and adiabatic index $\gamma = 1.4$, and an intense shock-wave with $M_0 = 4.5$ and $\gamma = 1.347$. For $M_0 = 1.75$ the flow of gas behind the shock-wave front is subsonic with Mach number $M_1 = 0.81$. As a result of the interaction with the cloud of particles the gas is slowed down and the particles are accelerated.

In Figs. 2-4 we show the velocity of the gas v_1 , the Mach number $M_1 = v_1/a$ and the pressure p as a function of the coordinate x at the instants of time $t_1 = 80 \mu\text{sec}$ and $t_2 = 160 \mu\text{sec}$ (curves 1 and 2) where $M_0 = 1.75$ (the vertical lines represent the left and right boundaries of the cloud). It can be seen from the figure that slowing down of a subsonic flow in a compression wave occurs in front of the cloud, while in the cloud itself it is accelerated in a rarefaction wave. The resultant slowing down is determined by the irreversible losses of the gas in the cloud due to friction and heat exchange.

After a time $t < 160 \mu\text{sec}$ the particles are no longer able to acquire velocity $v_2 \ll v_1$, and the cloud is hardly deformed. When $M_0 = 4.5$ the flow of gas behind the shock-wave front is supersonic ($M_1 = 1.86$), and the flow pattern that occurs differs qualitatively from the subsonic case.

In Figs. 5-7 we show v_1, M_1 and p as a function of x at the instants of time $t_1 = 40 \mu\text{sec}$ and $t_2 = 80 \mu\text{sec}$ (curves 1 and 2). The vertical lines indicate the left and right boundaries of the cloud at $t_1 = 40 \mu\text{sec}$ and $t_2 = 80 \mu\text{sec}$, corresponding to the coordinates x_i of the half-height of the cloud. The volume concentration m_2 as a function of x at the same instants of time is shown in Fig. 8, whence it follows that the cloud is slightly deformed when $t < 40 \mu\text{sec}$ and $M_0 = 4.5$. We can see from Figs. 5-7 that to the left of the cloud the flow is unperturbed, and slowing down of the gas occurs in the compression wave which is formed inside the cloud. Behind the cloud a rarefaction wave occurs in which the supercompressed gas is accelerated up to the final state, determined by the irreversible losses in the cloud. Hence, in the case of subsonic flow the gas

in the cloud is accelerated $\left[\frac{\partial v_1}{\partial x} > 0 \right]$, while in the case of supersonic flow it is slowed down $\left[\frac{\partial v_1}{\partial x} < 0 \right]$.

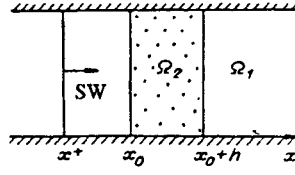


Fig. 1

3. To explain this effect we will investigate a simplified model in which we will neglect the motion of the particles. The equations of the flow of gas will then have the form

$$\begin{aligned}
 \frac{\partial \rho_1}{\partial t} + \rho_1 \frac{\partial v_1}{\partial x} + v_1 \frac{\partial \rho_1}{\partial x} &= 0, & \rho_1 &= \rho_{11} m_1, \\
 \rho_1 \left(\frac{\partial v_1}{\partial t} + v_1 \frac{\partial v_1}{\partial x} \right) &= -\frac{\partial p}{\partial x} - \frac{m_2 \rho_1 (v_1 - v_2)}{\tau}, \\
 T_1 \left(\frac{\partial S}{\partial t} + v_1 \frac{\partial S}{\partial x} \right) &= \frac{m_2 (v_1 - v_2)^2}{\tau} - \frac{m_2 (T_1 - T_2)}{\omega'}, \\
 S &= c_V \ln \frac{p}{\rho^\gamma} + S_0, & \tau &= \frac{\tau_0 \rho_{11}}{\rho_{22}},
 \end{aligned} \tag{3.1}$$

where S is the entropy and S_0 is a constant. Considering the effect of the cloud as a small perturbation, we will expand the required functions in series in powers of m_2^0 :

$$\varphi = \varphi_0 + \varphi', \quad \varphi = \{v_1, p, \rho_{11}, T_1, S\}. \tag{3.2}$$

Here φ_0 are the parameters of the gas behind the shock-wave and $\varphi \sim m_2^0$ are the corresponding perturbations. Substituting (3.2) into (3.1) and retaining terms in the first power of φ' we obtain

$$\begin{aligned}
 \frac{\partial \rho'}{\partial t} + \rho_0 \frac{\partial v'}{\partial x} + v_0 \frac{\partial \rho'}{\partial x} + \rho_0 v_0 \frac{d}{dx} (\ln m_1^0) &= 0, \\
 \frac{\partial v'}{\partial t} + v_0 \frac{\partial v'}{\partial x} + \frac{a_0^2}{\rho_0} \frac{\partial \rho'}{\partial x} + \frac{p_0}{c_V \rho_0} \frac{\partial S'}{\partial x} &= -\frac{m_2^0 v_0}{\tau}, \\
 \frac{\partial S'}{\partial t} + v_0 \frac{\partial S'}{\partial x} &= \frac{m_2^0 v_0^2}{\tau T_0} - \frac{m_2^0 (1 - T_2^0/T_1^0)}{\omega'}.
 \end{aligned}$$

Outside the region occupied by the particles we must put $m_2^0 = 0$. Introducing the dimensionless variables $\eta = \rho'/\rho_0$, $v = v'/v_0$, $s = S'/c_V$ and neglecting the term $\rho_0 v_0 \frac{d}{dx} (\ln m_1^0)$, in the equation of continuity, we obtain

$$\begin{aligned}
 \frac{1}{v_0} \frac{\partial \eta}{\partial t} + \frac{\partial \eta}{\partial x} + \frac{\partial v}{\partial x} &= 0, \\
 \frac{\partial v}{\partial t} + v_0 \frac{\partial v}{\partial x} + \frac{a_0^2}{v_0} \frac{\partial \eta}{\partial x} &= -\frac{a_0^2}{\gamma v_0} \frac{\partial s}{\partial x} - \int_{-\infty}^x \frac{m_2^0}{\tau} (\delta(y) - \delta(y-h)) dy, \\
 \frac{\partial s}{\partial t} + v_0 \frac{\partial s}{\partial x} &= m_2^0 \left(\frac{\gamma(\gamma-1)M^2}{\tau} - \frac{1 - T_2^0/T_1^0}{\omega} \right) \int_{-\infty}^x (\delta(y) - \delta(y-h)) dy, \\
 M &= \frac{v_0}{a_0}, \quad \tau = \frac{4}{3} \frac{d}{C_d v_0}, \quad \omega = \frac{d^2 \rho_{11}^0 c_V}{6 \lambda N u}.
 \end{aligned} \tag{3.3}$$

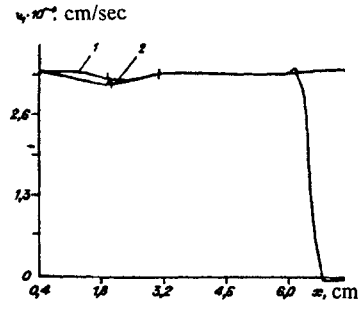


Fig. 2

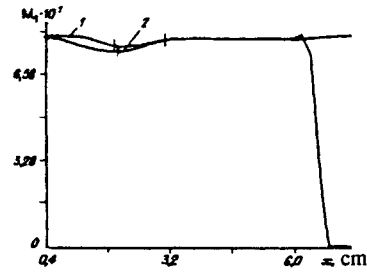


Fig. 3

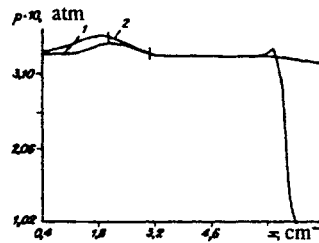


Fig. 4

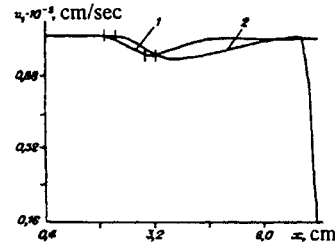


Fig. 5

The system of equations (3.3) holds over the whole region of the flow $-\infty < x < +\infty$, $t \geq 0$. The cloud of particles occupies the region $0 \leq x \leq h$. Outside the cloud the integral of the difference of the delta functions is equal to zero, while inside the cloud it is equal to unity. Multiplying the first equation by a_0 and combining it with the second we can reduce system (3.3) to the following characteristic form:

$$\frac{d^\pm J^\pm}{dt} = \varphi, \quad \frac{ds}{dt} = \psi, \quad J^\pm = v \pm \frac{a_0}{v_0} \eta, \quad (3.4)$$

where $\frac{d^\pm}{dt}$ and $\frac{d}{dt}$ are derivatives along the characteristics of C_\pm and C_0 :

$$C_\pm: \quad x = (v_0 \pm a_0)t + \xi_\pm, \quad C_0: \quad x = v_0 t + \xi_0. \quad (3.5)$$

The quantities φ and ψ were defined in (3.3)

$$\begin{aligned} \varphi &= \varphi_1 + \varphi_2, & \psi &= \psi_1 + \psi_2, \\ \varphi_1 &= -\frac{a_0^2}{\gamma v_0} \frac{\partial s}{\partial x}, & \varphi_2 &= -\frac{m_2^0}{\tau} \int_{-\infty}^x (\delta(y) - \delta(y-h)) dy, \\ \psi_1 &= m_2^0 \frac{\gamma(\gamma-1)M^2}{\tau} \int_{-\infty}^x (\delta(y) - \delta(y-h)) dy, \\ \psi_2 &= -m_2^0 \frac{1-T_2^0/T_1^0}{\omega} \int_{-\infty}^x (\delta(y) - \delta(y-h)) dy. \end{aligned}$$

Integrating system (3.4) taking into account the fact that $v|_{t=0} = \eta|_{t=0} = s|_{t=0} = 0$, we obtain

$$v = \frac{1}{2} \left(\int_{C_+} \varphi dt + \int_{C_-} \varphi dt \right), \quad s = \int_{C_0} \psi dt, \quad \eta = \frac{1}{2} \frac{v_0}{a_0} \left(\int_{C_+} \varphi dt - \int_{C_-} \varphi dt \right).$$

We will rewrite the integral $\int_{C_+} \varphi dt$ in the form $\int_{C_+} \varphi_1 dt + \int_{C_+} \varphi_2 dt$. By (3.5), $dx = (v_0 + a_0) dt$, along the C_+ -characteristic, and hence

$$\int_{C_+} \varphi_1 dt = \int_{\xi_+}^x \varphi_1 \frac{dx}{v_0 + a_0} = -\frac{a_0^2}{\gamma v_0(v_0 + a_0)} \int_{\xi_+}^x \frac{\partial s}{\partial x} dx = -\frac{a_0^2 s(t, x)}{\gamma v_0(v_0 + a_0)}, \quad (3.6)$$

where we have used the fact that $s(0, \xi_+) = 0$. Similarly, along the C_- -characteristic we obtain

$$\int_{C_-} \varphi_1 dt = -\frac{a_0^2 s(t, x)}{\gamma v_0(v_0 - a_0)}. \quad (3.7)$$

Substituting the integrals (3.6) and (3.7) into $\int_{C_{\pm}} \varphi dt$, we obtain

$$\begin{aligned} v &= -\frac{s}{\gamma(M^2 - 1)} - \frac{m_2^0}{2\tau} \left(\int_{C_+} \theta dt + \int_{C_-} \theta dt \right), \quad M = \frac{v_0}{a_0}, \\ \eta &= \frac{s}{\gamma(M^2 - 1)} - \frac{m_2^0}{2\tau} \left(\int_{C_+} \theta dt - \int_{C_-} \theta dt \right), \\ s &= \gamma(\gamma - 1)m_2^0 M^2 \int_{C_0} \theta \frac{dt}{\tau} - m_2^0 \left(1 - \frac{T_2^0}{T_1^0} \right) \int_{C_0} \theta \frac{dt}{\omega}, \\ \theta &= \begin{cases} 1 & \text{when } 0 \leq x \leq h, \\ 0 & \text{otherwise.} \end{cases} \end{aligned} \quad (3.8)$$

We will evaluate the integrals in (3.8) separately for subsonic ($M < 1$) and supersonic flow of the gas. The pattern of the characteristics is shown in Fig. 9 for $M < 1$. The half-plane $-\infty < x < +\infty$, $t > 0$ is divided by the lines Γ_i into 13 regions Ω_i . The equations for Γ_i are identical with the corresponding characteristics (3.5):

$$\begin{aligned} \Gamma_1: x &= (v_0 - a_0)t, & \Gamma_2: x &= (v_0 - a_0)t + h, \\ \Gamma_3: x &= v_0 t, & \Gamma_4: x &= v_0 t + h, \\ \Gamma_5: x &= (v_0 + a_0)t, & \Gamma_6: x &= (v_0 + a_0)t + h, \\ \Gamma_7: x &= 0, & \Gamma_8: x &= h. \end{aligned}$$

The points of intersection of the straight lines Γ_i have the coordinates

$$\begin{aligned} (x_A = \frac{h}{2}(1 + M), t_A = \frac{h}{2a_0}), & \quad (x_B = hM, t_B = \frac{h}{a_0}), \\ (x_C = 0, t_C = \frac{h}{a_0 - v_0}), & \quad (x_D = h, t_D = \frac{h}{a_0 + v_0}), \\ (x_E = h(1 + M), t_E = \frac{h}{a_0}), & \quad (x_F = h, t_F = \frac{h}{v_0}), \\ t_A &< t_D < t_B = t_E < t_F < t_C. \end{aligned}$$

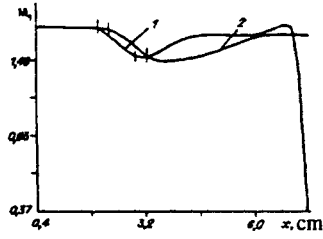


Fig. 6

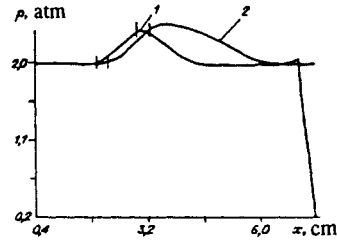


Fig. 7

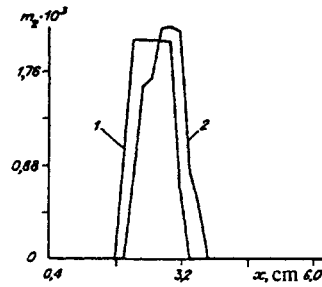


Fig. 8

We will construct, as an example, the solution in Ω_3 . Choosing the point G with coordinates x, t , we will evaluate the integrals in (3.8). We will denote by t_1 the instant when the characteristic C_0 intersects the straight line $x = 0$; we then have

$$\int_{C_0} \theta \frac{dt}{\tau} = \frac{t - t_1}{\tau} = \frac{x}{v_0 \tau}, \quad \int_{C_0} \theta \frac{dt}{\omega} = \frac{x}{v_0 \omega}.$$

Substituting these values into (3.8) we obtain

$$s = \gamma(\gamma - 1) \frac{m_2^0 x}{v_0 \tau} - m_2^0 \left(1 - \frac{T_2^0}{T_1^0}\right) \frac{x}{v_0 \omega} \quad \text{in } \Omega_3. \quad (3.9)$$

The integrals along C_+ and C_- have the form

$$\int_{C_+} \theta \frac{dt}{\tau} = \frac{t - t_2}{\tau} = \frac{x}{(v_0 + a_0)\tau}, \quad \int_{C_-} \theta \frac{dt}{\tau} = \frac{t - t_3}{\tau} = \frac{h - x}{(a_0 - v_0)\tau}.$$

Substituting these integrals into (3.8) and taking (3.9) into account we obtain

$$v' = -\frac{m_2^0 h M}{2\tau(1 - M)} + \frac{m_2^0 \gamma x M^2}{\tau(1 - M^2)} - \frac{m_2^0 x}{\gamma \omega(1 - M^2)} \frac{\Delta T}{T_1^0}, \quad (3.10)$$

where $\Delta T = T_1^0 - T_2^0$; $M < 1$. The integrals in the remaining regions Ω_i are evaluated similarly. As a result we obtain for the velocity v'

$$\begin{aligned}
v' &= -\frac{m_2^0 v_0}{2\tau} \left(t + \frac{x}{a_0 - v_0} \right) \quad \text{in } \Omega_1, \\
v' &= -\frac{m_2^0 h}{2\tau} \frac{M}{1 - M} \quad \text{in } \Omega_2, \\
v' &= -\frac{m_2^0 h}{2\tau} \frac{M}{1 + M} + \frac{m_2^0 h (\gamma - 1) M^2}{\tau (1 - M^2)} H \quad \text{in } \Omega_4, \\
v' &= -\frac{m_2^0 h}{2\tau} \frac{M}{1 + M} + \frac{m_2^0 (\gamma - 1) v_0 M^2}{\tau (1 - M^2)} \left(t - \frac{x - h}{v_0} \right) \quad \text{in } \Omega_5, \\
v' &= -\frac{m_2^0 h}{2\tau} \frac{M}{1 + M} \quad \text{in } \Omega_6, \\
v' &= -\frac{m_2^0 v_0}{2\tau} \left(t - \frac{x - h}{v_0 + a_0} \right) \quad \text{in } \Omega_7, \\
v' &= -m_2^0 v_0 \frac{t}{\tau} \left(1 - (\gamma - 1) \frac{M^2 H}{1 - M^2} \right) \quad \text{in } \Omega_8, \\
v' &= -\frac{m_2^0 v_0}{2\tau} \left(t + \frac{x}{v_0 + a_0} \right) + \frac{m_2^0 (\gamma - 1) x M^2 H}{\tau (1 - M^2)} \quad \text{in } \Omega_9, \\
v' &= -\frac{m_2^0 v_0}{2\tau} \left(t + \frac{x}{v_0 + a_0} \right) + \frac{m_2^0 v_0 (\gamma - 1) t M^2}{\tau (1 - M^2)} H \quad \text{in } \Omega_{10}, \\
v' &= -\frac{m_2^0 v_0}{2\tau} \left(t + \frac{h - x}{a_0 - v_0} \right) + \frac{m_2^0 v_0 (\gamma - 1) t M^2}{\tau (1 - M^2)} H \quad \text{in } \Omega_{11}, \\
v' &= -\frac{m_2^0 v_0}{2\tau} \left(t + \frac{h - x}{a_0 - v_0} \right) + \frac{m_2^0 v_0 (\gamma - 1) M^2}{\tau (1 - M^2)} \left(t + \frac{h - x}{v_0} \right) H \quad \text{in } \Omega_{12}, \\
v' &= -\frac{m_2^0 h}{2\tau} \frac{M}{1 - M} + \frac{m_2^0 x M^2}{\tau (1 - M^2)} + \frac{m_2^0 v_0 (\gamma - 1) t M^2}{\tau (1 - M^2)} H \quad \text{in } \Omega_{13}, \\
H &= 1 - \frac{\tau \Delta T}{\gamma (\gamma - 1) \omega T_1^0 M^2}, \quad M = \frac{v_0}{a_0} < 1, \quad \Delta T = T_1^0 - T_2^0.
\end{aligned} \tag{3.11}$$

It follows from Fig. 9 and Eq. (3.10) that when $t > t_c$ the flow of gas in the cloud will be steady and $a \, dv'/dx > 0$.

In Fig. 10 we show the qualitative relationship $v'(x)$ for a fixed instant t , drawn from Eqs. (3.10) and (3.11) (the vertical line represents the right-hand boundary of the cloud). It can be seen that $v'(x)$ agrees qualitatively with the calculated value. An exception is the region Ω_4 where $v' > 0$. However, as will be shown below, the value of $v'(x)$ in this region is small and does not exceed 0.5% of v_0 . The occurrence of $v' > 0$ is due to the effect of entropy, the contribution of which to v' , by (3.8), is $\Delta v'/v_0 = s/(\gamma(1 - M^2)) > 0$. A more accurate calculation of the heat exchange with the particles and the warm-up due to friction obviously leads to a reduction in $v'(x)$ in Ω_4 .

We will estimate the amplitude of the compression wave v_0' and the value of v_1' , equal to v' in Ω_4 (Fig. 10). Substituting into $\tau = 4/3 \, d/(C_d v_0)$, $\omega = d \text{Re Pr}/6v_0 \gamma \text{Nu}$ the values $\text{Re} = dv_0/\nu$, $\gamma = 1.4$, $\Delta T/T_1^0 \approx 0.5$, $M = 0.81$, $\text{Nu} \approx 0.6 \text{Re}^{1/2}$, $\text{Pr} \approx 0.66$, $d = 400 \, \mu\text{m}$ and $\nu = 0.15 \, \text{cm}^2/\text{sec}$, we obtain $v_1'/v_0 \approx 0.5\%$, $v_0'/v_0 \approx 4\%$. According to the numerical calculation presented in Fig. 2 the ratio $v_0'/v_0 \approx 6.1\%$, which agrees with the above estimate.

In the case of supersonic flow ($M_0 = 4.5$, $M_1 = 1.77$) the pattern of the characteristics has a different qualitative form (Fig. 11) where Γ_3, Γ_4 are identical with C_- , Γ_5, Γ_6 are identical with C_+ , and Γ_7, Γ_8 are identical with C_0 . The C_- -characteristics do not fall in the region to the left of the cloud, and hence the flow there remains unperturbed. The region of the solution is divided into thirteen subregions, separated by the straight lines Γ_i , which are described by the equations

$$\begin{aligned}
\Gamma_1 : \quad x &= 0, & \Gamma_2 : \quad x &= h, \\
\Gamma_3 : \quad x &= (v_0 - a_0)t, & \Gamma_4 : \quad x &= (v_0 - a_0)t + h, \\
\Gamma_5 : \quad x &= (v_0 + a_0)t, & \Gamma_6 : \quad x &= (v_0 + a_0)t + h, \\
\Gamma_7 : \quad x &= v_0 t, & \Gamma_8 : \quad x &= v_0 t + h.
\end{aligned}$$

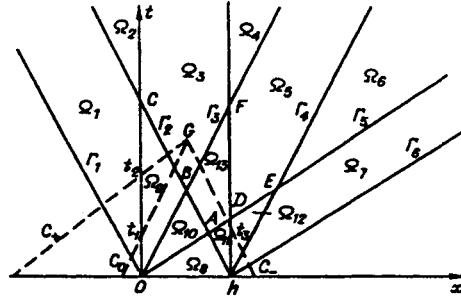


Fig. 9

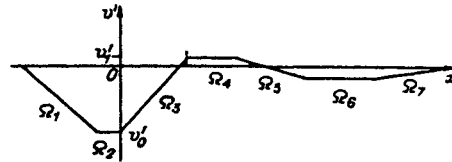


Fig. 10

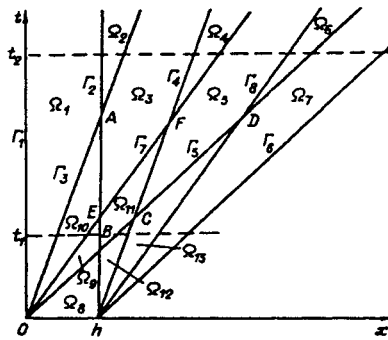


Fig. 11

The points of intersection of the straight lines Γ_i are as follows:

$$t_A = \frac{h}{v_0 - a_0}, \quad t_B = \frac{h}{v_0 + a_0}, \quad t_C = \frac{h}{2a_0},$$

$$t_D = \frac{h}{a_0}, \quad t_E = \frac{h}{v_0}, \quad t_F = \frac{h}{a_0}.$$

Since $M = v_0/a_0 > 1$, the following inequalities hold:

$$t_B < t_C < t_E < t_D = t_F < t_A.$$

The solution in the regions Ω_i is found from (3.8) and is constructed in the same way as (3.10). The sole difference is the fact that in this case we can neglect the heat exchange between the gas and the particles. (As an estimate shows, the increase in the entropy s due to friction, proportional to M^2 , considerably exceeds the reduction in s due to heat exchange.) As a result, the solution in the regions Ω_i has the form

$$\begin{aligned}
v' &= -\frac{m_2^0 x}{\tau} \frac{\gamma M^2}{M^2 - 1} \quad \text{in } \Omega_1, \\
v' &= -\frac{m_2^0 h}{\tau} \frac{\gamma M^2}{M^2 - 1} \quad \text{in } \Omega_2, \\
v' &= -\frac{m_2^0}{\tau} \left(h \frac{\gamma M^2}{M^2 - 1} + \frac{tv_0}{2} - \frac{xM}{2(M-1)} \right) \quad \text{in } \Omega_3, \\
v' &= -\frac{m_2^0}{\tau} \left(\frac{hM}{2(M+1)} + (\gamma-1) \frac{hM^2}{M^2-1} \right) \quad \text{in } \Omega_4, \\
v' &= -\frac{m_2^0}{\tau} \left(\frac{(\gamma-1)M^2}{M^2-1} (tv_0 + h - x) + \frac{hM}{2(M+1)} \right) \quad \text{in } \Omega_5, \\
v' &= -\frac{m_2^0 h}{2\tau} \frac{M}{M+1} \quad \text{in } \Omega_6, \\
v' &= -\frac{m_2^0 h}{2\tau} \left(\frac{M}{M+1} \left(1 - \frac{x}{h} \right) + \frac{tv_0}{h} \right) \quad \text{in } \Omega_7, \\
v' &= -\frac{m_2^0 tv_0}{\tau} \left(1 + \frac{(\gamma-1)M^2}{M^2-1} \right) \quad \text{in } \Omega_8, \\
v' &= -\frac{m_2^0}{2\tau} \left(\frac{2(\gamma-1)M^2}{M^2-1} tv_0 + tv_0 + \frac{Mx}{M+1} \right) \quad \text{in } \Omega_9, \\
v' &= -\frac{m_2^0}{2\tau} \left(\frac{2(\gamma-1)M^2}{M^2-1} x + tv_0 + \frac{Mx}{M+1} \right) \quad \text{in } \Omega_{10}, \\
v' &= -\frac{m_2^0}{2\tau} \left(\frac{2(\gamma-1)M^2}{M^2-1} (tv_0 + h - x) + \frac{2hM^2}{M^2-1} + tv_0 - \frac{Mx}{M-1} \right) \quad \text{in } \Omega_{11}, \\
v' &= -\frac{m_2^0}{\tau} \left(tv_0 \left(1 + \frac{(\gamma-1)M^2}{M^2-1} \right) - \frac{\gamma M^2}{M^2-1} (x - h) \right) \quad \text{in } \Omega_{12}, \\
v' &= -\frac{m_2^0}{2\tau} \left(\frac{2(\gamma-1)M^2}{M^2-1} (tv_0 + h - x) + tv_0 + \frac{M}{M+1} (h - x) \right) \quad \text{in } \Omega_{13}, \\
M &= \frac{v_0}{a_0} > 1.
\end{aligned} \tag{3.12}$$

In Fig. 12 we show the qualitative relationship $v'(x)$ at the instants of time $t_1, t_2, t_1 < t_2$ (see Fig. 11). It can be seen that the value of v' in the cloud decreases with time (the gas is slowed down), until, when $t > t_A$, a steady flow is established with a constant negative gradient $dv/dx < 0$. Outside the cloud the flow remains unsteady.

We will obtain the change in the Mach number in the cloud in the case of steady flow when $t > t_A$:

$$\frac{M}{M_0} = 1 + \frac{v'}{v_0} - \frac{a'}{a_0}, \quad M_0 = \frac{v_0}{a_0}. \tag{3.13}$$

Here, compared with (3.12) we have introduced new notation for the quantity $M_0 = \frac{v_0}{a_0}$, and a' is the perturbation of the velocity of sound $a = a_0 + a'$. From the equation of state of an ideal gas $p = B\rho^\gamma \exp(S/c_V)$ and the formula $a^2 = \left[\frac{\partial p}{\partial \rho} \right]_s$ we obtain the following expression for a' :

$$\frac{a'}{a_0} = \frac{s}{2} + \frac{\gamma-1}{2} \eta. \tag{3.14}$$

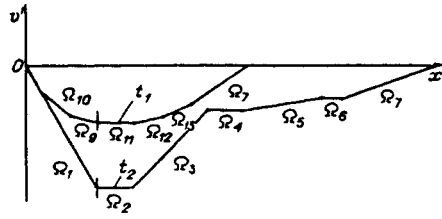


Fig. 12

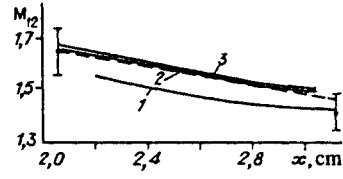


Fig. 13

The relations $\eta(x)$ and $s(x)$ are found from (3.8):

$$\eta = \gamma \frac{m_2^0 x}{\tau v_0} \frac{M_0^2}{M_0^2 - 1}, \quad s = \gamma(\gamma - 1) \frac{m_2^0 M_0^2 x}{v_0 \tau}. \quad (3.15)$$

Substituting (3.12), (3.14) and (3.15) into (3.13) we obtain

$$\frac{M}{M_0} = 1 - \frac{m_2^0 x}{\tau v_0} \frac{\gamma M_0^2}{M_0^2 - 1} \left(1 + \frac{\gamma - 1}{2} M_0^2\right). \quad (3.16)$$

Differentiating (3.16) with respect to x we obtain

$$\frac{dM}{dx} = -\frac{m_2^0}{\tau v_0} \frac{\gamma M_0^3}{M_0^2 - 1} \left(1 + \frac{\gamma - 1}{2} M_0^2\right).$$

The formula obtained is identical with the expression for dM/dx for the steady flow of a gas in a tube of constant cross section when there is friction [4].

The interaction between a shock-wave and a cloud of particles was investigated experimentally in [5, 6] for the same parameters of the gas and the particles as in this paper. The relative Mach number $M_{12} = |v_1 - v_2|/a$ was measured on the left-hand and right-hand boundaries of the cloud. The experimental results at the instant $t = 40 \mu\text{sec}$ are represented in Fig. 13 by the vertical lines, which indicate the spread in the experimental measurements. The spread arises due to the poly-dispersed nature and nonuniformity of the distribution of the particles in the cloud. The results of the numerical solution of the system of equations (1.1) are represented in Fig. 13 by the continuous curves: curve 1 corresponds to the fraction $d_1 = 170 \mu\text{m}$, curve 2 corresponds to the fraction $d_2 = 400 \mu\text{m}$, and curve 3 corresponds to the fraction $d_3 = 500 \mu\text{m}$. The dashed curves represent the results obtained using the formula

$$\Delta M = \sum_{i=1}^3 \Delta M_i, \quad \Delta M_i = M(m_2^{(i)}, d_i, x) - M_0,$$

where $M(m_2^{(i)}, d_i, x)$ is calculated from (3.16) with $\gamma = 1.4$, $C_d = 0.8$, $M_0 = 1.68$, $m_2^{(1)} = 5 \cdot 10^{-4}$, $d_1 = 170 \mu\text{m}$, $m_2^{(2)} = 10^{-3}$, $d_2 = 400 \mu\text{m}$, $m_2^{(3)} = 5 \cdot 10^{-4}$, and $d_3 = 500 \mu\text{m}$. It can be seen that the numerical and analytic solutions satisfactorily describe the experimental results.

REFERENCES

1. S. P. Kiselev, G. A. Ruev, A. P. Trunev, et al., Shock-Wave Processes in Two-Component and Two-Phase Media [in Russian], Nauka, Novosibirsk (1992).
2. S. P. Kiselev and V. M. Fomin, "A continuous-discrete model for gas-solid particle mixtures for a low volume concentration of the particles," Zh. Prikl. Mekh. Tekh. Fiz., No. 2, 93-101 (1986).

3. V. P. Kiselev, S. P. Kiselev, and V. M. Fomin, "The interaction between a shock wave and a cloud of particles of finite dimensions," *Zh. Prikl. Mekh. Tekh. Fiz.*, No. 2, 26-37 (1994).
4. L. G. Loitsyanskii, *Fluid and Gas Mechanics* [in Russian], Nauka, Moscow (1970).
5. V. M. Boiko, A. N. Papyrin, and S. V. Poplavskii, "The mechanism by which dust ignites in passing shock-wave," *Fiz. Goveniya Vznyva*, No. 3, 143-148 (1993).
6. S. V. Poplavskii, "Investigation of the nonstationary interaction between shock-wave and dust-gas mixtures," Candidate Dissertation, Novosibirsk (1992).